# Phe-Gly Dipeptidomimetics Designed for the Di-/Tripeptide Transporters PEPT1 and PEPT2: Synthesis and Biological Investigations

Jon Våbenø,[†] Tore Lejon,[||] Carsten Uhd Nielsen,[‡] Bente Steffansen,[‡] Weiqing Chen,[⊥] Hui Ouyang,[⊥] Ronald T. Borchardt,[⊥] and Kristina Luthman*[,†,§]

*Department of Medicinal Chemistry, Institute of Pharmacy, University of Tromsø, N-9037 Tromsø, Norway, Department of Chemistry, University of Tromsø, N-9037 Tromsø, Norway, Department of Pharmaceutics, The Danish University of Pharmaceutical Sciences, Universitetsparken 2, DK-2100 Copenhagen, Denmark, Department of Pharmaceutical Chemistry, The University of Kansas, Lawrence, Kansas 66047, and Department of Chemistry, Medicinal Chemistry, Göteborg University, SE−412 96 Göteborg, Sweden*

*Received September 5, 2003*

A series of five Phe-Gly dipeptidomimetics containing different amide bond replacements have been synthesized in a facile way from the readily available unsaturated ketoester **1**, and their affinities for the di-/tripeptide transporters hPEPT1 (Caco-2 cells) and rPEPT2 (SKPT cells) were tested. The compounds contained the amide bond isosteres ketomethylene (**2a**), (*R*)- and (*S*)-hydroxyethylidene (**3a** and **4a**), and (*R*)- and (*S*)-hydroxyethylene (**5a** and **6a**) to provide information on the conformational and stereochemical requirements for hPEPT1 and rPEPT2 affinity. The affinity studies showed that for rPEPT2 there is no significant difference in affinity between the ketomethylene isostere **2a** and the natural substrate Phe-Gly ($K_i$ values of 18.8 and 14.6 $\mu$M, respectively). Also the affinities for hPEPT1 are in the same range ($K_i$ values of 0.40 and 0.20 mM, respectively). This corroborates earlier findings that the amide bond as such is not essential for binding to PEPTX, but the results also reveal possible differences in the binding of ketomethylene isosteres to hPEPT1 and rPEPT2. The *trans*-hydroxyethylidene and hydroxyethylene isosteres proved to be poor substrates for PEPTX. These results provide new information about the importance of flexibility and of the stereochemistry at the $C_4$-position for this class of compounds. Furthermore, the intracellular uptake of **2a**−**4a** in Caco-2 cells was investigated, showing a 3-fold reduction of the uptake of **2a** in the presence of the competetive inhibitor Gly-Pro, indicating contribution from an active transport component. No active uptake of **3a** and **4a** was observed. Transepithelial transport studies also indicated active transport of **2a** across Caco-2 monolayers.

## Introduction

To ensure efficient amino acid absorption and conservation in the body, the intestine and kidneys are equipped with specific transport systems for di- and tripeptides. The di-/tripeptide transporter PEPT1 was first cloned from rabbit,[1] and both PEPT1[2] and PEPT2[3] (PEPTX) were cloned from human in 1995. PEPT1 is expressed in the intestinal brush border membrane,[2] while both PEPT1 and PEPT2 are expressed in the luminal membrane of the renal proximal tubule.[4,5] The main physiological role of intestinal PEPT1 is absorption of di- and tripeptides resulting from the enzymatic breakdown of dietary protein, while renal PEPT1 and PEPT2 both reabsorb di- and tripeptides from kidney filtrate.[6,7] The existence of peptide transporters, distinct from PEPT1 and PEPT2, in the basolateral membrane of both intestinal enterocytes[8−11] and renal tubule cells[12] have been suggested; however, none of these have yet been cloned. PEPT1 is often referred to as the low affinity/high capacity transporter, with substrate affinities in the mM-range, while PEPT2 is referred to as the high affinity/low capacity transporter, with substrate affinities in the $\mu$M-range.[13] The transport across the membrane has been shown to be a tertiary active process, driven by an $H^+$-gradient. PEPT1 has also been shown to play a role in the absorption of a wide variety of peptidomimetic drugs, such as $\beta$-lactam antibiotics[14] (penicillins and cephalosporins) and angiotensin converting enzyme (ACE) inhibitors.[15,16] Another therapeutic application of PEPT1 is the transport of amino acid prodrugs, such as valacyclovir[17] and valgancyclovir,[18] the L-valyl esters of acyclovir and gancyclovir, respectively. Other examples include the L-valyl ester of zidovudine (L-Val-AZT),[19] and amino acid prodrugs of methyldopa.[20,21] Likewise, dipeptides have been used as pro-moieties, and examples of this strategy include bisphosphonate prodrugs[22] and benzyl alcohol model prodrugs.[23]

The dipeptide prodrug approach has mainly been focused on the use of metabolically stable dipeptides (i.e. derivatives containing D-amino acids, imino acids, $\beta$-amino acids, etc.) as drug carriers. But as PEPT1 has a preference for the natural L,L-dipeptide skeleton,[24] such modifications will often make the resulting compound a poorer substrate. The possibilities for drug/prodrug delivery by targeting PEPT1 are promising, and bio-

* To whom correspondence should be addressed. Phone: +46−31−772−2894, fax: +46−31−772−3840, e-mail: luthman@chem.gu.se.
[†] Department of Medicinal Chemistry, University of Tromsø.
[||] Department of Chemistry, University of Tromsø.
[‡] The Danish University of Pharmaceutical Sciences.
[⊥] The University of Kansas.
[§] Göteborg University.

10.1021/jm031022+ CCC: $27.50 
Published on Web 01/06/2004

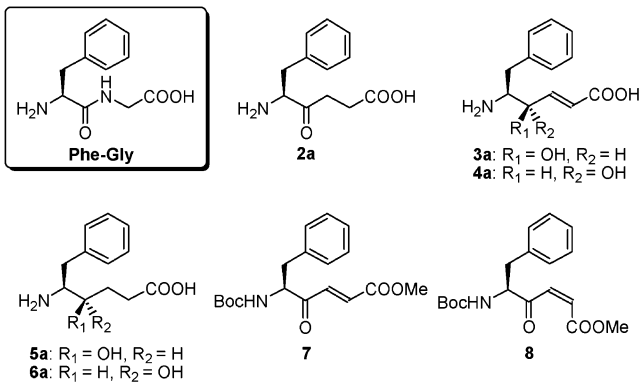


**Figure 1.** Structures of the synthesized Phe-Gly dipeptidomimetics.

pharmaceutical applications of this transport system have been extensively reviewed.[25−29] A peptidomimetic approach, where the scissile amide bond is replaced with different metabolically stable isosteric moieties, has the advantage of keeping the important structural features of the molecule comparable to that of the natural peptide (i.e. correct stereochemistry, correct distance between the *N*- and *C*-termini, etc.). However, there is still relatively limited information available on structure affinity (and hence, structure transport) relationships regarding PEPTX, and this approach requires more knowledge on which structural modifications of a peptide that are allowed without losing affinity for PEPTX. There are a few examples of compounds lacking an amide bond and still being substrates, e.g. compounds such as arphamenine A,[30] 4-aminophenylacetic acid (4-APAA),[31] $\delta$-amino levulinic acid,[32] and $\omega$-amino fatty acids,[33] indicating that the amide bond is not a prerequisite for transport. On the other hand, little is known about other amide bond isosteres and the importance of substrate flexibility.

Here we report the design, synthesis and biological evaluation of five Phe-Gly dipeptidomimetics (**2a**−**6a**, Figure 1) in which the amide bond has been replaced by isosteric moieties. To obtain structure−affinity information these replacements have been designed to mimic important properties of the amide bond, such as geometrical and/or electrostatic and hydrogen bonding properties. This series of compounds contains the ketomethylene isostere **2a**, and the *trans*-hydroxyethylidene (**3a** and **4a**) and hydroxyethylene (**5a** and **6a**) isosteres. Thus, the peptidomimetics **2a**−**6a** (Figure 1) are all of comparable size with the natural Phe-Gly dipeptide, have the correct stereochemistry, and a similar distance between the *N*- and *C*-termini. The compounds have been evaluated for their affinities and transport properties in vitro using the well-established Caco-2 (human PEPT1 transporter; hPEPT1) and SKPT (rat PEPT2 transporter; rPEPT2) cell assays.[34−37]

## Results and Discussion

**Chemistry.** The synthetic strategy is outlined in Scheme 1. We have earlier described the synthesis of the key intermediate **1**, and the chemo- and diastereoselective reduction of **1** to the unsaturated alcohols **3** and **4**.[38] Catalytic hydrogenation of the double bond in **1**, **3**, and **4** with $H_2$/Pd in EtOAc gave the saturated analogues **2**, **5**, and **6**, respectively, in high yields.

**Scheme 1**

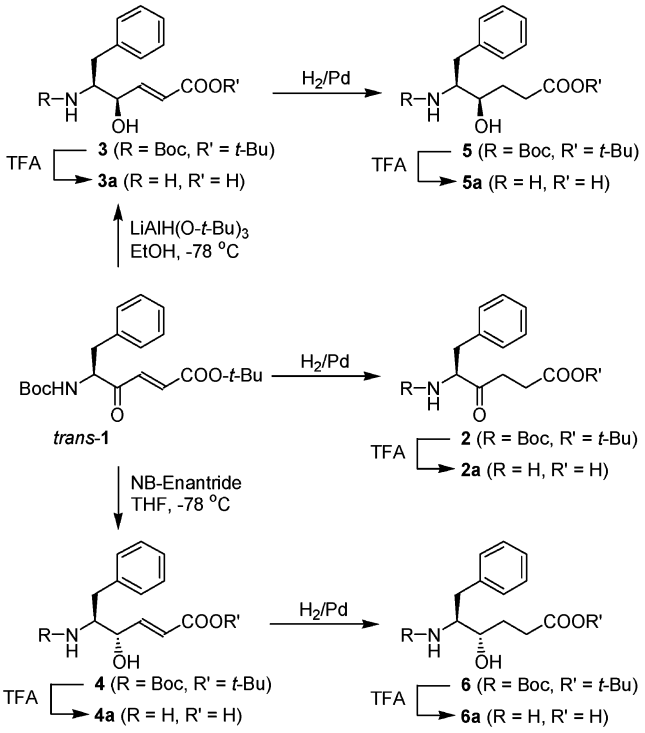


Catalytic hydrogenation of the corresponding methyl ester of **3** in EtOH has previously been reported to give the lactone as the only product.[39] This was not observed using the *tert*-butyl ester **3** in EtOAc, making this a very convenient strategy for obtaining both **5** and **6**. Deprotection of the *N*- and *C*-termini of **2**−**6** with TFA in $CH_2Cl_2$, followed by purification by reversed phase HPLC, afforded the trifluoroacetate salts of **2a**−**6a**.

To investigate the importance of the orientation of the carboxylate group, we originally intended to synthesize the fully deprotected, zwitterionic forms of the two unsaturated ketones *trans*-**1** and *cis*-**1** (*trans*- and *cis*-**1a**, respectively). To allow a one-step deprotection, the Boc-group and the *tert*-butyl ester were used as protecting groups. However, all attempts to deprotect **1** using TFA in $CH_2Cl_2$ failed. $^1$H NMR spectra of the crude product indicated degradation, probably due to rearrangements taking place in acidic media.

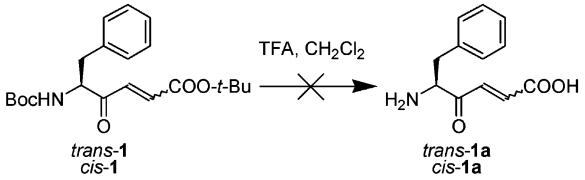


In an attempt to circumvent the problem of degradation of the unsaturated ketones, we decided to synthesize the methyl ester derivatives **7a** and **8a**. The methyl ester is more resistant to acidic hydrolysis and would supposedly make the final products more stable. At the same time the methyl group is fairly small and would provide compounds expected to act as substrates when tested for affinity to PEPTX. Compounds **7** and **8** were therefore synthesized analogously to the synthesis of **1**, but when an acidic *N*-deprotection was attempted (using TFA or MeOH/HCl(g)), we observed the same instability problems as with the *tert*-butyl esters.

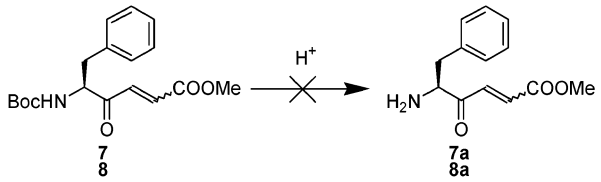


Rearrangements of this kind of compound under basic conditions are known from the literature,[40] and it seems as if a similar rearrangement can take place also in acidic media. Due to the failure to deprotect **7** and **8**, and their limited use as such due to solubility problems, these compounds were not included in the biological investigations.

**Biological Investigations.** The synthesized derivatives were tested for their affinity for PEPTX using Caco-2 and SKPT cell assays, and also for intracellular uptake and transepithelial transport via hPEPT1 (Caco-2 cells). Initial affinity screening of **2a**−**6a** for rPEPT2 in SKPT cells was performed in a relevant concentration range (0−1 mM)[13] (results not shown). The assay was based on inhibition of [$^{14}$C]-Gly-Sar uptake, and the results of this screen indicated that compound **2a** was a good substrate for PEPTX, whereas **3a**−**6a** were poor substrates. Approximations of the affinities of **3a**, **5a**, and **6a** (for compound **4a**, see below) were therefore based on inhibition of [$^{14}$C]-Gly-Sar uptake performed at a single high concentration (6 mM) for each compound, on both hPEPT1 in Caco-2 cells and rPEPT2 in SKPT cells. From the inhibition values, the concentrations required to inhibit the maximum uptake by 50% ($IC_{50}$ values) can be approximated (eq 2, see Experimental section). The inhibitory constant ($K_i$) values can then be calculated from the $IC_{50}$ values. A single interaction for the competitive interaction with Gly-Sar was obtained for all substrates investigated (Hill-factor n ≈ 1), and the maximum inhibition of [$^{14}$C]-Gly-Sar uptake, $U_{max}$, approached 1.0 (100%).

**A. Affinity of 2a−6a for rPEPT2 in SKPT Cells.** The affinities of **2a**−**6a** for rPEPT2 (SKPT-cells) were determined by their ability to inhibit the transport of [$^{14}$C]-Gly-Sar, a standard substrate for PEPTX. Phe-Gly and Phe-Ala were included in order to investigate the direct effect of an amide bond replacement.[41] For control purposes also the cephalosporin cephalexin, another standard substrate for PEPTX, was included. The Michaelis−Menten constant ($K_m$) of Gly-Sar for rPEPT2 was first determined to enable calculation of $K_i$ values of the compounds of interest (Figure 2). This was necessary because the SKPT cell assay used in this study is newly modified,[42] see Experimental section. The $K_m$ value of Gly-Sar was 110.4 ± 29.9 μM, with a maximum uptake rate ($V_{max}$) of 30.0 ± 3.5 pmol × cm$^{-2}$ × min$^{-1}$, which are comparable to the values obtained by Bravo et al.[42]

As compound **2a**, and to some extent compound **4a**, showed promising results in the initial screening, full affinity characterizations of these compounds in the concentration ranges 0−250 and 0−5000 μM, respectively, were undertaken. For the SKPT experiments, the Hill-factor *n* was in the range of 1.02−1.42, and $U_{max}$ was between 0.97 and 1.02. The results obtained demonstrate that the ketomethylene isostere **2a** has an affinity for rPEPT2 similar to those of the natural substrates Phe-Gly and Phe-Ala, and a higher affinity than cephalexin (Figure 3). An approximate 80-fold reduction in affinity is observed for compound **4a** (curve not shown), compared to **2a** (Table 1). The results for the other three compounds (Figure 4) show that **5a** and **6a** have approximately the same affinity, whereas **3a** has a somewhat higher affinity. The values correspond to an approximate 200-fold reduction in affinity for **3a** compared to **2a**, and a 400-fold reduction for both **5a** and **6a**.

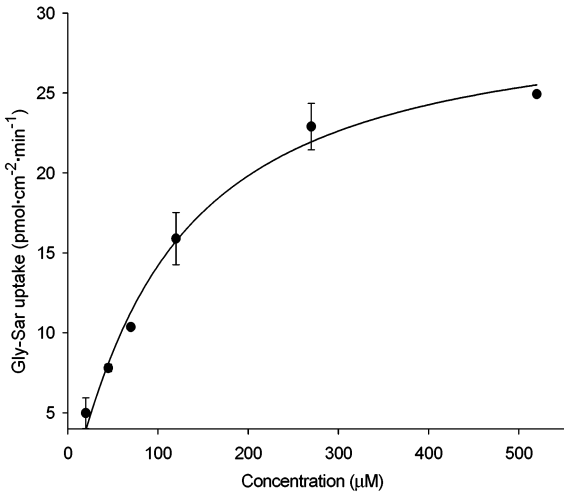


**Figure 2.** Uptake rate of Gly-Sar in SKPT-cells as a function of concentration.

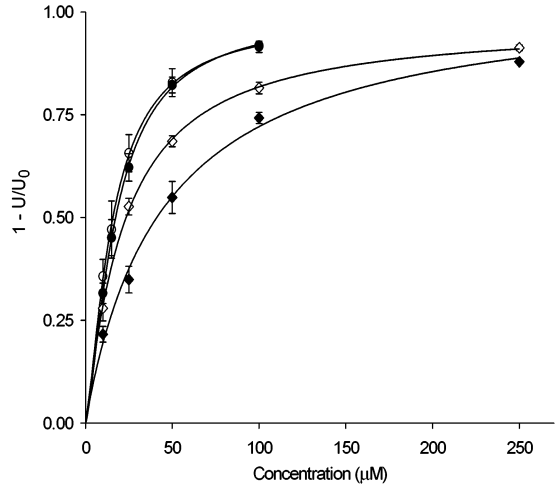


**Figure 3.** Inhibition of [$^{14}$C]-Gly-Sar uptake by Phe-Ala (○), Phe-Gly (●), **2a** (◇), and cephalexin (◆) in SKPT-cells. The lines describe the best fit to the experimentally obtained points using eq 2. Error bars represent SE.

**Table 1.** $IC_{50}$ and $K_i$ Values for rPEPT2 (SKPT cells)

| compound | $IC_{50}$ (μM) ± SE | $K_i$ (μM) |
|---|---|---|
| Phe-Gly | 17.2 ± 1.0 | 14.6 |
| Phe-Ala | 15.5 ± 0.9 | 13.1 |
| **2a** | 22.2 ± 2.4 | 18.8 |
| **3a** | 4111[a] | 3480[a] |
| **4a** | 1594 ± 360[b] | 1349 |
| **5a** | 8802[a] | 7451[a] |
| **6a** | 8176[a] | 6921[a] |
| cephalexin | 41.6 ± 5.1[b] | 35.2 |

[a] Estimated values. [b] Significantly different from Phe-Gly ($p < 0.05$).

**B. Affinity of 2a−6a for hPEPT1 in Caco-2 Cells.** Affinity determinations of **2a**−**6a** for hPEPT1 in con-

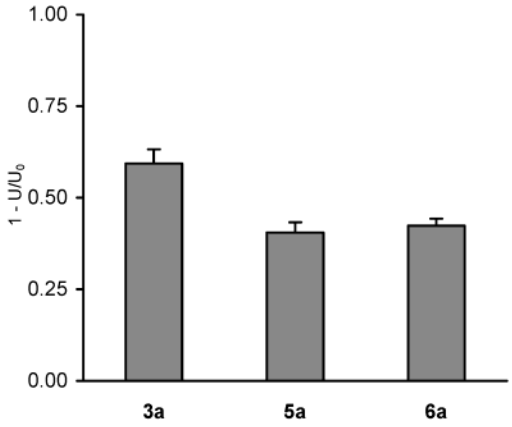


**Figure 4.** Relative reduction of [$^{14}$C]-Gly-Sar uptake in SKPT-cells in the presence of 6 mM of **3a**, **5a**, and **6a**, respectively. Error bars represent SE.

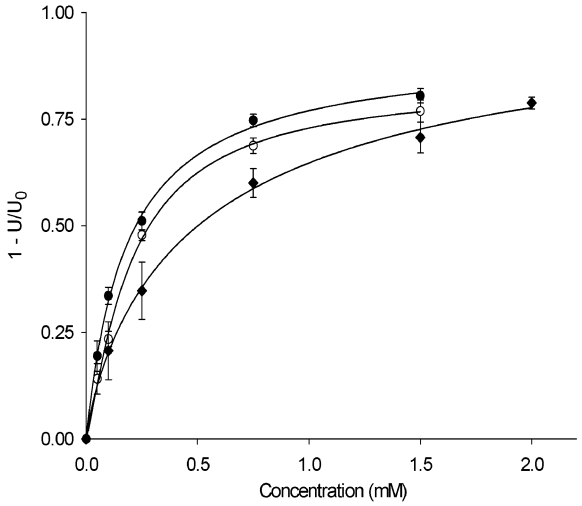


**Figure 5.** Inhibition of [$^{14}$C]-Gly-Sar uptake by Phe-Ala (●), Phe-Gly (○), and **2a** (◆) in Caco-2 cells. The lines describe the best fit to the experimentally obtained points using eq 2. Error bars represent SE.

**Table 2.** $IC_{50}$ and $K_i$ values for hPEPT1 (Caco-2 cells)

| compound | $IC_{50}$ (mM) ± SE | $K_i$ (mM) |
|---|---|---|
| Phe-Gly | 0.20 ± 0.02 | 0.20 |
| Phe-Ala | 0.18 ± 0.02 | 0.18 |
| **2a** | 0.40 ± 0.02[b] | 0.40 |
| **3a** | 26.8[a] | 26.4[a] |
| **4a** | 40.5[a] | 39.8[a] |

[a] Estimated values. [b] Significantly different from Phe-Gly ($p$ < 0.01).

fluent mature Caco-2 cell monolayers were carried out in the same manner, also including Phe-Gly and Phe-Ala. For compound **2a**, a full characterization was undertaken over a concentration range of 0−2 mM. For the Caco-2 experiments, the Hill-factor $n$ was in the range of 0.83−1.21, and $U_{max}$ was between 0.84 and 1.05. The results (Figure 5) demonstrate that there is a 2-fold difference in $K_i$ values between the natural substrates (Phe-Gly and Phe-Ala) and the ketomethylene isostere **2a** (Table 2). The unsaturated alcohols **3a** and **4a** inhibit Gly-Sar uptake to a small extent at a concentration of 6 mM, whereas the saturated analogues **5a** and **6a** have a negligible effect at this concentration (Figure 6). As the values for **5a** and **6a** were in the same range as the standard error (SE), no

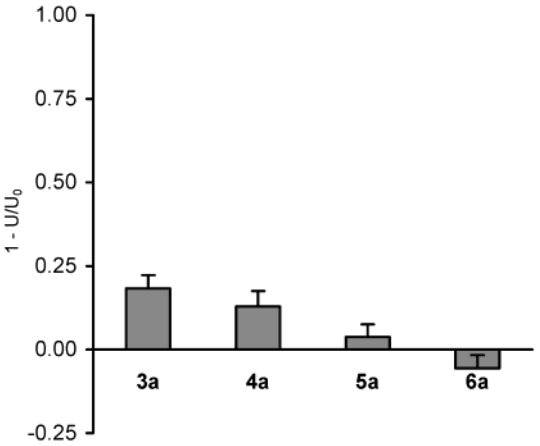


**Figure 6.** Relative reduction of [$^{14}$C]-Gly-Sar uptake in Caco-2 cells in the presence of 6 mM of **3a**, **4a**, **5a**, and **6a**, respectively. Error bars represent SE.

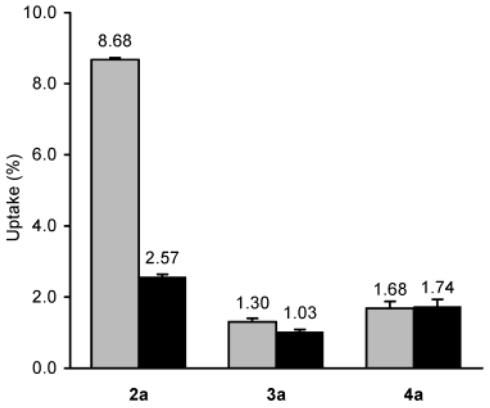


**Figure 7.** Intracellular uptake (in percent of total amount added) of 0.5 mM **2a**−**4a** in Caco-2 cells in absence (gray) and presence (black) of 5 mM Gly-Pro. Error bars represent SE.

attempts were made to estimate $IC_{50}$ values for these two compounds.

**C. Intracellular Uptake Studies of 2a−4a in Caco-2 Cells.** As affinity studies only give information about binding to the transporter, intracellular uptake studies in Caco-2 cells were carried out to investigate the actual translocation by hPEPT1. To demonstrate active transport, these experiments were carried out in absence and presence (10-fold excess) of the known competetive PEPTX inhibitor Gly-Pro. The results (Figure 7) show a 3-fold reduction ($p$ < 0.01) in the uptake of **2a** in the presence of the inhibitor, indicating that this compound is transported by hPEPT1. For **3a** and **4a** the uptake is low, and no difference in uptake is observed when Gly-Pro is added, indicating that no active uptake is taking place.

**D. Transepithelial Transport Studies of 2a−4a across Caco-2 Cell Monolayers.** Transepithelial transport studies were subsequently carried out to investigate the overall transport across the cell monolayer. These experiments were also carried out in the absence and presence (20-fold excess) of Gly-Pro. As the transepithelial transport is a result of several processes, it is difficult to separate the individual transport components, which means that these results must be treated with caution. As shown in Figure 8, the inclusion of Gly-Pro in the incubation media caused a significant reduction ($p$ < 0.01) in the apparent permeability coefficients

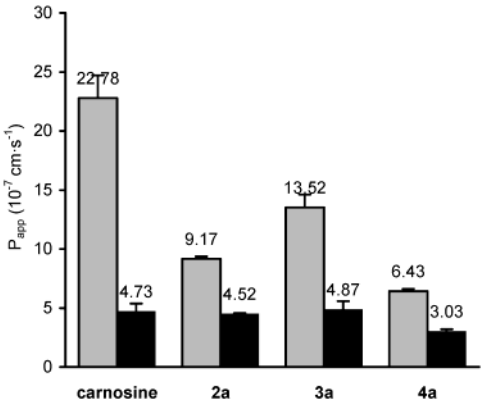


**Figure 8.** Transepithelial transport of 0.5 mM carnosine and **2a**−**4a** across Caco-2 monolayers in absence (gray) and presence (black) of 10 mM Gly-Pro. Error bars represent SE.

($P_{app}$) for all four compounds (carnosine, **2a**, **3a**, **4a**). For **2a**, the transepithelial transport data (Figure 8) are consistent with the uptake data (Figure 7), which suggested that transport of this compound across the apical membrane of Caco-2 cell monolayers was at least partially transporter-mediated. From the data shown in Figure 8 it is difficult to draw any conclusions about the mechanism(s) (passive diffusion and/or active transport) by which **2a** permeates the cells' basolateral membrane. The transepithelial transport data (Figure 8) for **3a** and **4a**, particularly the inhibitory effect of Gly-Pro on their transport, are not consistent with the cellular uptake data shown in Figure 7, as these uptake data suggest that **3a** and **4a** are entering the cells across the apical membrane by passive diffusion (i.e. their uptake is not inhibited by Gly-Pro). A possible explanation for this apparent discrepancy is that while the apical uptake of these two compounds proceeds via passive diffusion, their efflux out of the cell across the basolateral membrane is partially mediated by the basolateral peptide transporter. Even if the basolateral transporter is suggested to be distinct from the apical transporter hPEPT1,[9] it is likely to be sensitive to inhibition by intracellular Gly-Pro.[43] Considering the polar nature of all three compounds studied (i.e. **2a**, **3a**, and **4a**), the paracellular pathway of transepithelial transport may also be contributing significantly to the $P_{app}$ values reported in Figure 8, particularly when the transport experiments were done in the presence of Gly-Pro.

L-Carnosine is a well-known substrate for hPEPT1; however, there are conflicting results in the literature regarding the transepithelial transport of this compound. Due to its stability, L-carnosine has been widely used as a reference compound,[24,44] and according to the results of these studies, the inhibitory effect of Gly-Pro on the transepithelial transport of L-carnosine shown in Figure 8 could be expected. In contrast, a recent kinetic study showed that the transepithelial transport of L-carnosine across Caco-2 cell monolayers followed apparent simple nonsaturable kinetics, indicative of passive transport, but the study confirmed at the same time that the transport across both the apical and basolateral membrane was carrier-mediated.[45] The above-mentioned studies illustrate the complexity in giving a mechanistic interpretation of the data shown in Figure 8. The results derived from these experiments could vary depending on the relative importance of passive diffusion and carrier-mediated transport of the compound under study, its relative substrate activity for transporters in the apical and basolateral membranes of Caco-2 cells, and the relative affinity of Gly-Pro for these transporters. Surprisingly, **5a** and **6a** showed high $P_{app}$ values in these studies (results not shown). However, considering their polar nature and their low affinities for hPEPT1, this is most likely due to paracellular transport.

**Structure−Affinity Relationships.** 3D structures of mammalian peptide transporter proteins have not yet been established, and the only way to extract structure−affinity information for the transporter is by ligand-based design. Several models for binding to the transporter have been suggested. Recently, a template model was proposed in a review by Rubio-Aliaga and Daniel,[46] but essentially the same template was earlier proposed by Bailey et al.[47] This latter model also indicated the relative orientation of the groups of the peptide considered important for interaction with PEPT1. According to this model, there are four important structural features for dipeptides: (1) the positively charged *N*-terminus, (2) the negatively charged *C*-terminus, (3) the amide carbonyl oxygen, and (4) the interaction of the $R_2$ side chain with a proposed hydrophobic pocket.[48] In addition, Bailey et al.[47] suggest that the bond to the terminal carboxylate group of a dipeptide should be oriented 60° relative to the plane of the amide bond. The amide NH functionality does not seem to be involved in any direct interaction with the transporter. Although this model is based on data obtained from different test systems, it currently remains the most comprehensive model for describing affinity for PEPT1. It should be emphasized that none of the four 'critical' features highlighted in the model of Bailey et al. are absolute prerequisites for affinity, as substrates lacking one of these may still have affinity. The model therefore in essence describes an ideal substrate.[49]

The replacement of the enzymatically labile amide bond of Phe-Gly with the stable ketomethylene isostere of **2a** results in a loss of H-bond donor properties as well as in an increased flexibility, since the partial double bond character of the amide is lost. From the results it is seen that this replacement reduces the apparent affinity for hPEPT1 approximately 2-fold, whereas the apparent affinity for rPEPT2 is not significantly changed.

When going from the planar carbonyl group of **2a** to the tetrahedral alcohol of **3a**−**6a**, additional molecular properties are altered, most importantly the geometry, but also the H-bonding properties and charge distribution of the molecule. The affinity studies showed a pronounced reduction in affinity for the alcohols **3a**−**6a** compared to the ketone **2a**, both for hPEPT1 and rPEPT2. One would expect higher desolvation energies for the alcohols compared to the ketone, but this is not sufficient to explain this large difference.

Regarding the hydrogen bonding potential, the alcohols **3a**−**6a** have both H-bond donor and acceptor properties. However, the position of the donor (OH-group) make them less appropriate as replacements for the NH group of the amide bond if interaction with a H-bond acceptor in the transporter is of importance. All the peptidomimetics have an oxygen-containing func-

tionality at $C_4$, which can act as a H-bond acceptor. However, the orientation of the oxygen atom in space will be quite different, and the planar carbonyl group of **2a** obviously gives this compound more favorable binding properties compared to the alcohol derivatives. It is difficult to dissect the precise molecular property that causes this dramatic change, since this difference possibly originates from a combination of geometrical and electrostatic properties. In any case the results demonstrate the importance of a planar, polarized $C_4$−O bond.

The affinities of the alcohols were lower than what we consider interesting for pro-moieties useful for active transport by hPEPT1 (∼15 mM). For hPEPT1 there seems to be no difference in affinity between the (4*S*)-alcohols **4a** and **6a** and their respective (4*R*)-epimers **3a** and **5a**, whereas the unsaturated (4*S*)-alcohol **4a** shows an approximate 2.5-fold increase in affinity for rPEPT2 compared to its (4*R*)-epimer **3a**. This indicates that even though these compounds are not ideal substrates, the orientation of the oxygen at $C_4$ has some implication for the affinity.

According to the model of Bailey et al., the more flexible dipeptidomimetics **2a**, **5a**, and **6a** should be preferred as substrates as they may adopt the required conformation, positioning the N- and C-termini in the correct spatial arrangement. However, the results obtained showed that the hydroxyethylene isosteres **5a** and **6a** generally had lower affinity than their unsaturated counterparts, both for hPEPT1 and rPEPT2. This was unexpected, since the trans-double bond in the allylic alcohols **3a** and **4a** would prevent these derivatives from adopting the required torsional angle of approximately 60°. Although these compounds are not ideal substrates for PEPTX, it can be concluded from these experiments that the torsional freedom is not a prerequisite for binding.

There are striking differences between the low affinity/high capacity hPEPT1 and the high affinity/low capacity rPEPT2. For the natural substrates Phe-Gly and Phe-Ala, there is an approximate 10-fold reduction in affinity for hPEPT1 compared to rPEPT2, and this effect is even more pronounced for **2a**, which has a 20-fold reduction. It should be born in mind that hPEPT1 and rPEPT2 in this study are of human and rat origin, respectively, and that species differences in part can contribute to this observation. But this could also indicate that PEPT1 discriminates between substrates to a larger extent than PEPT2.

**Structure−Transport Relationships for hPEPT1.** The ketomethylene isostere **2a** is the only compound that shows active intracellular uptake (Figure 7). Since these experiments were done at a concentration of 0.5 mM, one would not expect the hydroxyethylidene isosteres **3a** and **4a** to show any significant active uptake because of their weak affinities.

In the case of active transepithelial transport the basolateral transporter also comes into play. From the transepithelial transport studies (Figure 8) it appears as compounds **3a** and **4a** are actively transported, but as they are not actively taken up into the cell (Figure 7), the overall transport cannot be purely carrier-mediated. Thus, it is difficult to draw conclusions regarding the structural requirements for the basolateral transporter. For compound **2a**, which shows active uptake, the results from the transepithelial transport studies imply an overall active transport component.

## Conclusions

A series of structurally related Phe-Gly dipeptidomimetics were shown to provide important information on the structure−affinity and structure−transport relationships for PEPTX transport systems. The affinity studies show that the metabolically stable ketomethylene isostere **2a** has an affinity comparable to the natural substrate Phe-Gly, whereas the hydroxyethylidene and hydroxyethylene isosteres are poor substrates for both isoforms of the peptide transporter. As compound **2a** also shows active uptake into Caco-2 cells, this implies that this is a promising pro-moiety for a prodrug approach targeting hPEPT1, and such studies are presently ongoing in our laboratory.

## Experimental Section

**Chemistry. General.** Starting materials and reagents were purchased from Sigma, Fluka, Aldrich, and Merck KGaA, and were used as received. $^1$H and $^{13}$C NMR spectra were recorded on a Varian Mercury Plus operating at 400 and 100 MHz, respectively. Chemical shifts are given relative to the solvent signal ($\delta$ 7.26 and $\delta$ 77.0 for $CDCl_3$, and $\delta$ 3.49 and $\delta$ 49.0 for $CD_3OD$, respectively). TLC was performed using silica gel coated aluminum sheets (silica gel 60 $F_{254}$, Merck), with visualization by UV detection and/or 5% phosphomolybdic acid hydrate (PMA) in EtOH, followed by heating. Flash chromatography was performed on silica gel (silica gel 60 (0.040−0.063 mm), Merck) under nitrogen pressure. THF was distilled from Na/benzophenone ketyl. Other solvents were of analytical or synthetic grade and were used without further purification. Melting points were taken with a Büchi Melting Point B-540 apparatus and are uncorrected. Optical activity was measured using a Perkin-Elmer 241 Polarimeter. Elemental analyses were done by Mikro Kemi AB, Uppsala, Sweden. In HPLC a Gilson 115 UV detector (254 nm) and a Waters 510 pump were used. Normal phase analytical chromatography for compounds **1**−**8** was performed on a LiChrosorb Si 60 (5 $\mu$m) 4 × 250 mm analytical column from Merck KgaA (flow rate 1.0 mL/min). Reversed phase analytical chromatography for compounds **2a**−**6a** was performed on a Symmetry Shield $RP_{18}$ (3.5 $\mu$m) 2.1 × 150 mm analytical column from Waters (isocratic: 12% $CH_3CN$, 0.1% TFA; flow rate 0.2 mL/min). Normal phase preparative chromatography of compounds **3** and **4** was performed on a Prep Nova-Pak HR Silica 6 $\mu$m 60 Å 25 × 100 mm column from Waters (flow rate 6.0 mL/min). Reversed phase preparative chromatography of compounds **2a**−**6a** was performed on a Prep Nova-Pak HR C18 6 $\mu$m 60 Å 25 × 100 mm column from Waters (isocratic: 20% $CH_3CN$, 0.1% TFA; flow rate 7.0 mL/min). The syntheses of **1**, **3**, **4**,[38] and **7**[39] have been described earlier.

**General Procedure for Reduction of the Double Bond (synthesis of 2, 5, and 6).** A 130 mg amount of unsaturated compound was dissolved in EtOAc (15 mL), 10% Pd/C (15 mg) was added, and the mixture was stirred under $H_2$ atmosphere overnight. The mixture was filtered through Celite to remove the catalyst, and the filtrate was concentrated under reduced pressure. Flash chromatography of the residue gave the pure product.

***tert*-Butyl (5*S*)-5-[*N*-(*tert*-Butoxycarbonyl)amino]-4-oxo-6-phenyl-hexanoate (2).** Flash chromatography [$Et_2O$:pentane 2:1] gave **2** (83 mg, 64%) as a white solid; mp 78−81 °C; $[\alpha]_D$ +25.5° (*c* 1.94, $CHCl_3$); analytical HPLC: $t_R$ 6.61 min (1% EtOH in *iso*-hexane); $^1$H NMR ($CDCl_3$) $\delta$ 7.29−7.15 (m, 5H), 5.11 (d, 1H, $J$ = 7.2 Hz), 4.53 (app q, 1H), 3.12 (dd, 1H, $J$ = 14.0, 6.0 Hz,), 2.93 (dd, 1H, $J$ = 14.2, 7.0 Hz), 2.69 (t, 2H, $J$ = 6.8 Hz), 2.47 (t, 2H, $J$ = 6.6 Hz), 1.42 (s, 9H), 1.38 (s, 9H). $^{13}$C NMR ($CDCl_3$) $\delta$ 207.8, 172.0, 155.5, 136.5, 129.5 (2 C:s),

128.8 (2 C:s), 127.2, 80.9, 80.0, 60.4, 37.7, 35.4, 29.2, 28.5 (3 C:s), 28.3 (3 C:s). Anal. ($C_{21}H_{31}NO_5$) C, H, N.

***tert*-Butyl (4*R*,5*S*)-5-[*N*-(*tert*-Butoxycarbonyl)amino]-4-hydroxy-6-phenyl-hexanoate (5).** Flash chromatography [$Et_2O$:pentane 1:1] gave **5** (106 mg, 81%) as a white solid; mp 140−142.5 °C; $[\alpha]_D$ −7.1° (*c* 1.01, $CHCl_3$); analytical HPLC: $t_R$ 9.40 min (2% EtOH in *iso*-hexane); $^1$H NMR ($CDCl_3$) $\delta$ 7.31−7.19 (m, 5H), 4.66 (br d, 1H), 3.85 (br s, 1H), 3.64 (br d, 1H), 3.57 (br s, 1 H), 2.95−2.74 (m, 2H), 2.51−2.37 (m, 2H), 1.87−1.68 (m, 2H) 1.45 (s, 9H), 1.35 (s, 9H). $^{13}$C NMR ($CDCl_3$) $\delta$ 174.1, 156.5, 138.3, 129.5 (2 C:s), 128.7 (2 C:s), 126.6, 80.9, 79.9, 73.8, 56.9, 36.1, 32.6, 28.5, 28.3 (6 C:s). Anal. ($C_{21}H_{33}NO_5$) C, H, N.

***tert*-Butyl (4*S*,5*S*)-5-[*N*-(*tert*-Butoxycarbonyl)amino]-4-hydroxy-6-phenyl-hexanoate (6).** Flash chromatography [$Et_2O$:pentane 1:1] gave **6** (110 mg, 84%) as a white solid; mp 54−57 °C; $[\alpha]_D$ −7.2° (*c* 1.49, $CHCl_3$); analytical HPLC: $t_R$ 9.40 min (2% EtOH in *iso*-hexane); $^1$H NMR ($CDCl_3$) $\delta$ 7.30−7.18 (m, 5H), 4.98 (br d, 1H), 3.75−3.69 (m, 1H), 3.56 (br d, 1H), 3.42 (br s, 1 H), 2.94−2.84 (m, 2H), 2.42−2.27 (m, 2H), 1.86−1.63 (m, 2H) 1.40 (s, 9H), 1.39 (s, 9H). $^{13}$C NMR ($CDCl_3$) $\delta$ 174.3, 156.4, 138.7, 129.6 (2 C:s), 128.7 (2 C:s), 126.5, 81.1, 79.5, 71.2, 56.4, 38.9, 32.7, 29.9, 28.6 (3 C:s), 28.2 (3 C:s). Anal. ($C_{21}H_{33}NO_5$) C, H, N.

**Methyl (5*S*)-5-[*N*-(*tert*-Butoxycarbonyl)amino]-4-oxo-6-phenyl-(*E*)-2-hexenoate (7) and Methyl (5*S*)-5-[*N*-(*tert*-Butoxycarbonyl)amino]-4-oxo-6-phenyl-(*Z*)-2-hexenoate (8).** The two isomers were synthesized analogously to **1**,[38] using methyl glyoxylate instead of *tert*-butyl glyoxylate. Starting from 1.09 g (2.94 mmol) of dimethyl [(3*S*)-3-[*N*-(*tert*-butoxycarbonyl)amino]-2-oxo-4-phenyl-butyl]phosphonate, flash chromatography of the crude product [$Et_2O$:pentane 2:1] gave pure **7** (520 mg) and **8** (132 mg) as light yellow solids in a total yield of 66%. For spectroscopical data on **7**, see ref 39. **8**: mp 91−93 °C; $[\alpha]_D$ −44.8° (*c* 1.13, $CHCl_3$); analytical HPLC: $t_R$ 7.70 min (1% EtOH in *iso*-hexane); $^1$H NMR ($CDCl_3$) $\delta$ 7.31−7.18 (m, 5H), 6.44 (d, 1H, $J$ = 12.0 Hz), 6.06 (d, 1H, $J$ = 11.6 Hz), 5.13 (br d, 1H, $J$ = 8.4 Hz), 4.72 (app q, 1H), 3.75 (s, 3H), 3.25 (dd, 1H, $J$ = 14.2, 5.8 Hz), 3.01 (dd, 1H, $J$ = 14.2, 7.4 Hz), 1.39 (s, 9H). $^{13}$C NMR ($CDCl_3$) $\delta$ 201.9, 166.1, 155.5, 139.9, 136.7, 129.6 (2 C:s), 128.8 (2 C:s), 127.1, 126.4, 80.2, 60.8, 52.5, 37.4, 28.5 (3 C:s). Anal. ($C_{18}H_{23}NO_5$) C, H, N.

**Deprotection. General Procedure for 2−6.** The protected compound was dissolved in $CH_2Cl_2$ (2 mL), and TFA (0.4 mL) was added. The mixture was stirred at room temperature for 2 h, and $Et_2O$ (10 mL) was added and evaporated three times. The crude mixture was dissolved in 3 mL of mobile phase and purified with reversed phase preparative HPLC. The combined fractions were evaporated under reduced pressure. Freeze-drying of the aqueous residue gave the final products.

**(5*S*)-5-Amino-4-oxo-6-phenyl-hexanoic Acid (2a).** Compound **2** (73 mg) gave **2a** (56.2 mg, 87%) as a white solid; mp 115 °C (dec); $[\alpha]_D$ +41.7° (*c* 0.95, MeOH); analytical HPLC: $t_R$ 5.9 min; $^1$H NMR ($CD_3OD$) $\delta$ 7.41−7.31 (m, 5H), 4.46 (dd, 1H, $J$ = 8.6, 5.8 Hz), 3.40 (dd, 1H, $J$ = 14.6, 5.4 Hz), 3.00 (dd, 1H, $J$ = 14.4, 8.4 Hz,), 2.88−2.72 (m, 2H), 2.62 (app t, 2H). $^{13}$C NMR ($CD_3OD$) $\delta$ 204.5, 174.6, 134.5, 129.3 (2 C:s), 129.1 (2 C:s), 127.8, 59.8, 35.8, 34.4, 27.3. Anal. ($C_{12}H_{15}NO_3$·TFA) C, H, N.

**(4*R*, 5*S*)-5-Amino-4-hydroxy-6-phenyl-(*E*)-2-hexenoic Acid (3a).** Compound **3** (62 mg) gave **3a** (44 mg, 81%) as a colorless semisolid; $[\alpha]_D$ +22.0° (*c* 1.09, MeOH); analytical HPLC: $t_R$ 5.5 min; $^1$H NMR ($CD_3OD$) $\delta$ 7.37−7.26 (m, 5H), 6.95 (dd, 1H, $J$ = 15.6, 4.4 Hz), 6.18 (dd, 1H, $J$ = 15.6, 2.0 Hz), 4.55−4.53 (m, 1H), 3.71−3.67 (m, 1H), 2.95 (dd, 1H, $J$ = 14.4, 6.0 Hz), 2.86 (dd, 1H, $J$ = 14.4, 8.8 Hz). $^{13}$C NMR ($CD_3OD$) $\delta$ 168.2, 144.5, 135.8, 129.2 (2 C:s), 128.9 (2 C:s), 127.3, 124.1, 69.1, 56.7, 33.7. Anal. ($C_{12}H_{15}NO_3$·TFA) C, H, N.

**(4*S*, 5*S*)-5-Amino-4-hydroxy-6-phenyl-(*E*)-2-hexenoic Acid (4a).** Compound **4** (61 mg) gave **4a** (50 mg, 92%) as a colorless semisolid; $[\alpha]_D$ −5.6° (*c* 0.89, MeOH); analytical HPLC: $t_R$ 5.9 min; $^1$H NMR ($CD_3OD$) $\delta$ 7.38−7.27 (m, 5H), 6.86 (dd, 1H, $J$ = 15.2, 4.8 Hz), 6.17 (dd, 1H, $J$ = 15.4, 1.8 Hz), 4.29−4.27 (m, 1H), 3.54−3.49 (m, 1H), 3.09 (dd, 1H, $J$ = 13.6, 8.0 Hz), 2.95 (dd, 1H, $J$ = 13.8, 7.0 Hz). $^{13}$C NMR ($CD_3OD$) $\delta$ 168.1, 146.3, 135.7, 129.3 (2 C:s), 128.9 (2 C:s), 127.4, 124.0, 67.9, 56.1, 35.8. Anal. ($C_{12}H_{15}NO_3$·TFA) H, N; C: calcd, 50.15; found, 49.7.

**(4*R*, 5*S*)-5-Amino-4-hydroxy-6-phenyl-hexanoic Acid (5a).** Compound **5** (98 mg) gave **5a** (76.6 mg, 88%) as a white solid; mp 70 °C (dec); $[\alpha]_D$ −31.1° (*c* 1.0, MeOH); analytical HPLC: $t_R$ 5.7 min; $^1$H NMR ($CD_3OD$) $\delta$ 7.41−7.28 (m, 5H), 4.76−4.71 (m, 1H), 3.92−3.87 (m, 1H), 3.10 (dd, 1H, $J$ = 14.4, 6.0 Hz), 2.89 (dd, 1H, $J$ = 14.4, 8.4 Hz), 2.74−2.53 (m, 2H), 2.45−2.37 (m, 1H), 2.18−2.08 (m, 1H). $^{13}$C NMR ($CD_3OD$) $\delta$ 176.8, 134.9, 129.2 (2 C:s), 129.1 (2 C:s), 127.6, 78.7, 54.4, 33.4, 27.8, 22.5. Anal. ($C_{12}H_{17}NO_3$·1.5 TFA): C, H, N.

**(4*S*, 5*S*)-5-Amino-4-hydroxy-6-phenyl-hexanoic Acid (6a).** Compound **6** (98 mg) gave **6a** (70 mg, 81%) as a colorless semisolid; $[\alpha]_D$ +19.5° (*c* 2.16, MeOH); analytical HPLC: $t_R$ 5.6 min; $^1$H NMR ($CD_3OD$) $\delta$ 7.40−7.29 (m, 5H), 4.61−4.55 (m, 1H), 3.71−3.65 (m, 1H), 3.07 (dd, 1H, $J$ = 14.0, 6.8 Hz), 2.97 (dd, 1H, $J$ = 14.4, 7.2 Hz), 2.71−2.52 (m, 2H), 2.36−2.28 (m, 1H), 2.06−1.96 (m, 1H).$^{13}$C NMR ($CD_3OD$) $\delta$ 176.6, 134.6, 129.4 (2 C:s), 129.1 (2 C:s), 127.6, 79.1, 55.7, 35.3, 27.9, 24.9. Anal. ($C_{12}H_{17}NO_3$·0.75TFA) C, N; H: calcd, 5.80; found, 5.2.

**Cell Assays. A. Materials. General.** Caco-2 cells for the affinity, uptake, and transport assays were obtained from the American Type Culture Collection (Manassas, VA). SKPT-0193 cl.2 (SKPT) cells were donated by Dr. Matthias Brandsch (Biozentrum, Halle, Germany) with kind permission of Dr. Ulrich Hopfer (Case Western Reserve University, Cleveland, OH). All chemicals for buffer preparations were of laboratory grade, obtained from Life Technologies and Sigma. Transwell plates (12-well and 6-well) were from Corning Costar Corporation. **Affinity Studies.** Phe-Gly and Phe-Ala were from Bachem, and [$^{14}$C]-Gly-Sar (specific activity: 49.94 mCi/mmol) and [$^3$H]-mannitol (specific activity: 51.50 mCi/mmol) were from New England Nuclear. Transepithelial electrical resistance (TEER) was measured in tissue resistance measurement chambers (Endohm) with a voltohmmeter (EVOM), both from World Precision Instruments. The shaking plate used for cell culture experiments was a KS 10 DIGI shaker from Edmund Bühler. Radioactivity was determined in a Packard TriCarb liquid scintillation counter, using Ultima Gold scintillation fluid from Packcard. **Uptake and Transport Studies.** Gly-Pro and L-carnosine were obtained from Sigma, and [$^{14}$C]-mannitol from Amersham. The centrifuge was from IEC and the sonicator from Cole Parmer Instrument Company. For HPLC, a Shimadzu SPD-6A UV detector (210 nm), a Shimadzu LC-6A pump, and a Vydac 218TP54, 5 $\mu$M, 250 × 4.6 mm analytical column were used.

**B. Cell Culture.** Caco-2 cells for affinity experiments were cultured as previously described.[50] Briefly, cells were seeded in culture flasks and passaged in Dulbecco's Modified Eagle's medium (DMEM) supplemented with 10% fetal bovine serum, penicillin/streptomycin (100 U/mL and 100 $\mu$g/mL, respectively), 1% L-glutamine and 1% nonessential amino acids. Caco-2 cells were seeded onto tissue culture treated 12-well Transwell plates (1.0 cm$^2$, 0.4 $\mu$m pore size) at a density of $10^5$ cells × cm$^{-2}$. Monolayers were grown in an atmosphere of 5% $CO_2$ − 95% $O_2$ at 37 °C. Growth media were replaced every other day. Dipeptide transport activity reached a steady maximum level at day 24−30. Affinity experiments were subsequently performed on day 26−28 after seeding. TEER at room temperature was measured in each well before the experiment, and the mean ± standard deviation (SD) was 382.3 ± 41 Ω × cm$^{-2}$ ($n$ = 21). The TEER value of a filter support without cells is typically 27 Ω × cm$^{-2}$.

SKPT-cells were cultured as described by Bravo et al.[42] Briefly, cells at passage 44 were seeded in culture flasks and passaged in 1:1 DMEM/Nutrient mixture F-12 (F12). The culture media were supplemented with 10% fetal bovine serum, 100 U/mL penicillin, 100 $\mu$g/mL streptomycin, 5 mg/mL insulin, 4 mg/mL dexamethasone, and 5 mg/mL apotransferrin. When cells reached passages 45−63, they were seeded onto tissue culture treated 12-well Transwell plates (1 cm$^2$,

0.4 mm pore size), at a density of $5 \times 10^6$ cells/cm$^2$. Monolayers were grown in an atmosphere of 5% $CO_2$−95% $O_2$ at 37 °C. Growth media were replaced every other day. Dipeptide transport activity reached a steady maximum level at day 3−5. Affinity experiments were subsequently performed on day 3−4 after seeding. TEER at room temperature was measured in each well before the experiment. The mean ± SD was 5.00 ± 0.94 ($n$ = 15) and 7.56 ± 1.01 ($n$ = 9) on day 3 and 4, respectively, giving an overall mean of 5.96 ± 1.57 kΩ × cm$^{-2}$.

Caco-2 cells for the uptake and transport experiments were maintained for 21 days in 6-well Transwell plates as described earlier.[51] For the transport experiments the integrity of the monolayers was checked using [$^{14}$C]-mannitol. The $P_{app}$ values of [$^{14}$C]-mannitol across Caco-2 cell monolayers were typically in the range of 0.1−0.6 × $10^{-6}$ cm/s.

**C. Glycylsarcosine Uptake Experiments.** For SKPT-cells, uptake of [$^{14}$C]-Gly-Sar was measured in Hanks Balanced Salt Solution (HBSS) supplemented with 0.05% bovine serum albumin (BSA). Apical media were buffered with 10 mM 2-[*N*-morpholino]ethanesulfonic acid (MES) buffer, and pH was adjusted to 6.0. Basolateral media were buffered with 10 mM *N*-[2-hydroxyethyl]piperazine-*N*′-[2-ethanesulfonate] (HEPES) buffer and adjusted to pH 7.4. Cells were placed on a shaking plate, preheated to 37 °C, and allowed to equilibrate for 15 min in apical and basolateral buffer solutions. The experiment was started by adding fresh apical buffer containing the relevant Gly-Sar concentration (0−500 μM) and 0.5 μCi [$^{14}$C]-Gly-Sar per well. 0.5 μCi [$^3$H]-mannitol per well was added to the apical solution, as a marker of extracellular space. Uptake experiments were terminated after 30 min by gentle suction of the uptake medium, followed by three washes of the monolayers with ice-cold HBSS. Following the washing step, the cells were cut from the Transwell support and placed into scintillation vials, and 2 mL of scintillation fluid was added. The cell-associated radioactivity was counted via liquid scintillation spectrometry.

For Caco-2 cells, a $K_m$ value of 1.1 mM obtained in our laboratory was used for Gly-Sar, and concentration dependent Gly-Sar uptake was not investigated further.

**D. Affinity Studies.** The buffers used for affinity studies were the same as for Gly-Sar uptake, as was the equilibration time and conditions. The affinity experiment was initiated by adding 0.5 mL of MES-buffer containing 0.5 μCi of [$^{14}$C]-Gly-Sar and various amounts of the respective compounds to the apical side. For SKPT-cells, 0.5 μCi of [$^3$H]-mannitol per well was also added to the apical solution, as a marker of extracellular space. A 1.0 mL amount of HEPES buffer was added to the basolateral side of each cell monolayer. Previous results in our laboratory showed that uptake in Caco-2 cells was linear up to 6−7 min of incubation, and thus the incubation time was 5 min. For SKPT-cells, the uptake has been shown to be linear for >60 min, and the incubation time was 30 min. During incubation the plates were circularly and continuously shaken. In all experiments the investigated compounds were only applied on the apical side. The temperature was maintained at 37 °C. The uptake of 0.5 μCi [$^{14}$C]-Gly-Sar was terminated by gentle suction of the uptake medium followed by three washes of the monolayer with ice-cold HBSS. The filter supports were cut out, and the cell-associated radioactivity was determined.

For affinity studies of **3a**−**6a** (Caco-2 cells) and **3a**, **5a**, and **6a** (SKPT-cells), the same procedure was used, however only at one concentration (6 mM) of the compound.

**E. Intracellular Uptake in Caco-2 Cells.** Caco-2 cells were maintained for 21 days in 6-well Transwell plates. Prior to the initiation of the uptake study, cell monolayers were washed twice with HBSS (pH 7.35) and incubated in HBSS for 20 min at 37 °C. After removing HBSS on both apical and basolateral sides, 0.5 mM of the peptide analogue in 1500 μL of Earle's balanced salt solution (EBSS) (pH 6.0), with or without the presence of 5 mM of Gly-Pro, was applied to the apical side. Fresh HBSS was then applied to the basolateral side of each well. Cell monolayers were incubated for another 60 min at 37 °C and then washed three times with ice-cold HBSS. The cells on polyester membrane were harvested into 1.5 mL centrifuge vials, spun down, redissolved in 300 μL of water, and sonicated for 2 min. The cell preparation was extracted with 300 μL of $CH_2Cl_2$, and a 200 μL sample was taken from the aqueous phase. After acidification using 100 μL of 0.05 N HCl, the sample was analyzed by HPLC (isocratic; 10% $CH_3CN$; flow rate 1.0 mL/min).

**F. Transepithelial Transport across Caco-2 Cell Monolayers.** Prior to initiation of the transport experiments, cell monolayers were washed twice with HBSS (pH 7.35) and incubated in HBSS at 37 °C for 20 min. Then, 2.5 mL of fresh HBSS (pH 7.35) was applied to the basolateral side of each well, and 1.5 mL of peptide analogue solution (500 μM in EBSS, pH 6.0), with or without 10 mM of Gly-Pro, was applied to the apical side of each well. Samples were taken from the basolateral side at intervals up to 90 min and analyzed by HPLC (isocratic; 10% $CH_3CN$; flow rate 1.0 mL/min).

**G. Data Analysis. 1. Transport Kinetics. A. Uptake of Gly-Sar.** Uptake of Gly-Sar in SKPT-cells was corrected for noncellular uptake, and the cellular uptake as a function of apical Gly-Sar concentration was fitted to a Michaelis−Menten type equation:

$$V = \frac{V_{max} \times [S]^n}{{K_m}^n + [S]^n} \quad (1)$$

where $V$ = uptake rate (pmol × cm$^{-2}$ × min$^{-1}$), $V_{max}$ = maximum uptake rate (pmol × cm$^{-2}$ × min$^{-1}$), $K_m$ = the Michaelis−Menten constant (μM), [S] = Gly-Sar concentration (μM), and $n$ = Hill-factor.

**B. Affinity.** Affinity for hPEPT1 and rPEPT2 in Caco-2 and SKPT-cells, respectively, was determined as inhibition of [$^{14}$C]-Gly-Sar uptake in the presence of varying concentrations of the respective compound. The degree of inhibition was fitted to a Michaelis−Menten type equation:

$$1 - (U/U_0) = \frac{(1 - (U/U_0))_{max} \times [I]^n}{{IC_{50}}^n + [I]^n} \quad (2)$$

where $U$ = uptake of [$^{14}$C]-Gly-Sar, $U_0$ = uptake of [$^{14}$C]-Gly-Sar at zero inhibitor concentration, $IC_{50}$ = the concentration required to inhibit the maximum uptake by 50% (μM or mM), [I] = compound concentration (μM or mM), and $n$ = Hill-factor. When estimating $IC_{50}$ values for compounds which were tested at only one concentration, the Hill-factor, $n$, was assumed to equal 1 and the expression $(1 - (U/U_0))_{max}$ was assumed to be 1 based on the results obtained for the other compounds. $K_i$ values were calculated as described by Cheng and Prusoff.[52]

**C. Intracellular Uptake.** The percent uptake of peptide analogue was calculated using:

$$\text{uptake (\%)} = \frac{Q_{retained}}{Q_{total}} \times 100 \quad (3)$$

where $Q_{retained}$ is the amount retained in the cell monolayer and $Q_{total}$ is the total amount added to each well.

**D. Transepithelial Transport.** The $P_{app}$ values of the compounds were calculated by:

$$P_{app} = \frac{\Delta Q/\Delta t}{A \times C_0} \quad (4)$$

where $\Delta Q/\Delta t$ is the linear appearance rate of mass in the receiver solution, $A$ is the cross-section area (4.71 cm$^2$), and $C_0$ is the initial concentration of the donor side at $t = 0$.

**2. Statistics Analysis.** Unless stated otherwise, values are given as means ± SE, and the statistical significance of the results was determined using two-tailed Students $t$-test (or Welch's corrected t-test when means with different variances were compared) using GraphPad InStat v3.05. $p < 0.05$ was considered significant. Affinity experiments on both Caco-2 and SKPT-cell monolayers were done in duplicates in each passage

($N = 2$), and $n$ was the number of cell passages used ($n = 3$). Uptake and transport experiments were done in triplicates ($n = 3$).

**Acknowledgment.** Financial support for this project was obtained from the Norwegian Research Council (128256/420), the Swedish Science Research Council (621-2001-1431), the Knut and Alice Wallenberg Foundation (98.176), and the Danish Medicinal Research Council via the Center for Drug Design and Transport and via project grant #22-01-0310. This research has also been supported by a Marie Curie Fellowship of the European Community Program "Improving the Human Research Potential and the Socio-Economic Knowledge Base" under contract number HPMT-CT-2001-00403. We thank Kjell H. Halvorsen for excellent assistance in the synthetic work, Morten Moe for assistance with preparative and analytical HPLC, Dr. Bengt Erik Haug for assistance with the freeze-drying, and Susanne N. Sørensen for doing the cell culturing.

## References

(1) Fei, Y. J.; Kanai, Y.; Nussberger, S.; Ganapathy, V.; Leibach, F. H.; Romero, M. F.; Singh, S. K.; Boron, W. F.; Hediger, M. A. Expression cloning of a mammalian proton-coupled oligopeptide transporter. *Nature* **1994**, *368*, 563−566.

(2) Liang, R.; Fei, Y. J.; Prasad, P. D.; Ramamoorthy, S.; Han, H.; Yang-Feng, T. L.; Hediger, M. A.; Ganapathy, V.; Leibach, F. H. Human intestinal $H^+$/peptide cotransporter. Cloning, functional expression, and chromosomal localization. *J. Biol. Chem.* **1995**, *270*, 6456−6463.

(3) Liu, W.; Liang, R.; Ramamoorthy, S.; Fei, Y. J.; Ganapathy, M. E.; Hediger, M. A.; Ganapathy, V.; Leibach, F. H. Molecular cloning of PEPT 2, a new member of the $H^+$/peptide cotransporter family, from human kidney. *Biochim. Biophys. Acta* **1995**, *1235*, 461−466.

(4) Smith, D. E.; Pavlova, A.; Berger, U. V.; Hediger, M. A.; Yang, T.; Huang, Y. G.; Schnermann, J. B. Tubular localization and tissue distribution of peptide transporters in rat kidney. *Pharm. Res.* **1998**, *15*, 1244−1249.

(5) Boll, M.; Herget, M.; Wagener, M.; Weber, W. M.; Markovich, D.; Biber, J.; Clauss, W.; Murer, H.; Daniel, H. Expression cloning and functional characterization of the kidney cortex high-affinity proton-coupled peptide transporter. *Proc. Natl. Acad. Sci. U.S.A.* **1996**, *93*, 284−289.

(6) Ganapathy, V.; Leibach, F. H. Carrier-mediated reabsorption of small peptides in renal proximal tubule. *Am. J. Physiol. Renal Physiol.* **1986**, *251*, F945−953.

(7) Daniel, H.; Morse, E.; Adibi, S. The high and low affinity transport systems for dipeptides in kidney brush border membrane respond differently to alterations in pH gradient and membrane potential. *J. Biol. Chem.* **1991**, *266*, 19917−19924.

(8) Dyer, J.; Beechey, R. B.; Gorvel, J. P.; Smith, R. T.; Wootton, R.; Shirazi-Beechey, S. P. Glycyl-L-proline transport in rabbit enterocyte basolateral-membrane vesicles. *Biochem. J.* **1990**, *269*, 565−571.

(9) Saito, H.; Inui, K. Dipeptide transporters in apical and basolateral membranes of the human intestinal cell line Caco-2. *Am. J. Physiol.* **1993**, *265*, G289-G294.

(10) Thwaites, D. T.; Brown, C. D. A.; Hirst, B. H.; Simmons, N. L. Transepithelial glycylsarcosine transport in intestinal Caco-2 cells mediated by expression of hydrogen ion-coupled carriers at both apical and basal membranes. *J. Biol. Chem.* **1993**, *268*, 7640−7642.

(11) Terada, T.; Sawada, K.; Saito, H.; Hashimoto, Y.; Inui, K. Functional characteristics of basolateral peptide transporter in the human intestinal cell line Caco-2. *Am. J. Physiol.* **1999**, *276*, G1435−1441.

(12) Terada, T.; Sawada, K.; Ito, T.; Saito, H.; Hashimoto, Y.; Inui, K.-I. Functional expression of novel peptide transporter in renal basolateral membranes. *Am. J. Physiol. Renal Physiol.* **2000**, *279*, F851−857.

(13) For $K_i$ values of typical substrates for PEPTX, including peptides; see ref 29 and references therein.

(14) Bretschneider, B.; Brandsch, M.; Neubert, R. Intestinal transport of $\beta$-lactam antibiotics: Analysis of the affinity at the $H^+$/peptide symporter (PEPT1), the uptake into Caco-2 cell monolayers and the transepithelial flux. *Pharm. Res.* **1999**, *16*, 55−61.

(15) Moore, V. A.; Irwin, W. J.; Timmins, P.; Lambert, P. A.; Chong, S.; Dando, S. A.; Morrison, R. A. A rapid screening system to determine drug affinities for the intestinal dipeptide transporter 2: affinities of ACE inhibitors. *Int. J. Pharm.* **2000**, *210*, 29−44.

(16) For a review with other examples of pharmacologically active compounds with affinity for/transport by PepT1, see ref 25 and references therein.

(17) de Vrueh, R. L. A.; Smith, P. L.; Lee, C. P. Transport of L-valine-acyclovir via the oligopeptide transporter in the human intestinal cell line, Caco-2. *J. Pharmacol. Exp. Ther.* **1998**, *286*, 1166−1170.

(18) Sugawara, M.; Huang, W.; Fei, Y. L.; Leibach, F. H.; Ganapathy, V.; Ganapathy, M. E. Transport of valganciclovir, a ganciclovir prodrug, via peptide transporters PEPT1 and PEPT2. *J. Pharm. Sci.* **2000**, *89*, 781−789.

(19) Han, H. K.; de Vrueh, R. L. A.; Rhie, J. K.; Covitz, K. M. Y.; Smith, P. L.; Lee, C. P.; Oh, D. M.; Sadee, W.; Amidon, G. L. 5′-Amino acid esters of antiviral nucleosides, acyclovir, and AZT are absorbed by the intestinal PEPT1 peptide transporter. *Pharm. Res.* **1998**, *15*, 1154−1159.

(20) Hu, M.; Subramanian, P.; Mosberg, H. I.; Amidon, G. L. Use of the peptide carrier system to improve the intestinal absorption of L-α-methyldopa: Carrier kinetics, intestinal permeabilities, and in vitro hydrolysis of dipeptidyl derivatives of L-α-methyldopa. *Pharm. Res.* **1989**, *6*, 66−70.

(21) Bai, P. F.; Subramanian, P.; Mosberg, H. I.; Amidon, G. L. Structural requirements for the intestinal mucosal-cell peptide transporter: The need for N-terminal α-amino group. *Pharm. Res.* **1991**, *8*, 593−599.

(22) Ezra, A.; Hoffman, A.; Breuer, E.; Alferiev, I. S.; Monkkonen, J.; El Hanany-Rozen, N.; Weiss, G.; Stepensky, D.; Gati, I.; Cohen, H.; Tormalehto, S.; Amidon, G. L.; Golomb, G. A peptide prodrug approach for improving bisphosphonate oral absorption. *J. Med. Chem.* **2000**, *43*, 3641−3652.

(23) Taub, M. E.; Moss, B. A.; Steffansen, B.; Frokjaer, S. Oligopeptide transporter mediated uptake and transport of D-Asp(OBzl)-Ala, D-Glu(OBzl)-Ala, and D-Ser(Bzl)-Ala in filter-grown Caco-2 monolayers. *Int. J. Pharm.* **1998**, *174*, 223−232.

(24) Tamura, K.; Bhatnagar, P. K.; Takata, J. S.; Lee, C. P.; Smith, P. L.; Borchardt, R. T. Metabolism, uptake, and transepithelial transport of the diastereomers of Val-Val in the human intestinal cell line, Caco-2. *Pharm. Res.* **1996**, *13*, 1213−1218.

(25) Brodin, B.; Nielsen, C. U.; Steffansen, B.; Frøkjær, S. Transport of peptidomimetic drugs by the intestinal di/tri-peptide transporter, PepT1. *Pharmacol. Toxicol.* **2002**, *90*, 285−296.

(26) Bai, J. P. F.; Amidon, G. L. Structural specificity of mucosal-cell transport and metabolism of peptide drugs: Implication for oral peptide drug delivery. *Pharm. Res.* **1992**, *9*, 969−978.

(27) Yang, C. Y.; Dantzig, A. H.; Pidgeon, C. Intestinal peptide transport systems and oral drug availability. *Pharm. Res.* **1999**, *16*, 1331−1343.

(28) Walter, E.; Kissel, T.; Amidon, G. L. The intestinal peptide carrier: A potential transport system for small peptide derived drugs. *Adv. Drug Delivery Rev.* **1996**, *20*, 33−58.

(29) Nielsen, C. U.; Brodin, B.; Jorgensen, F. S.; Frokjaer, S.; Steffansen, B. Human peptide transporters: therapeutic applications. *Expert Opin. Ther. Pat.* **2002**, *12*, 1329−1350.

(30) Enjoh, M.; Hashimoto, K.; Arai, S.; Shimizu, M. Inhibitory effect of arphamenine A on intestinal dipeptide transport. *Biosci. Biotechnol. Biochem.* **1996**, *60*, 1893−1895.

(31) Temple, C. S.; Stewart, A. K.; Meredith, D.; Lister, N. A.; Morgan, K. M.; Collier, I. D.; Vaughan-Jones, R. D.; Boyd, C. A. R.; Bailey, P. D.; Bronk, J. R. Peptide mimics as substrates for the intestinal peptide transporter. *J. Biol. Chem.* **1998**, *273*, 20−22.

(32) Döring, F.; Walter, J.; Will, J.; Focking, M.; Boll, M.; Amasheh, S.; Clauss, W.; Daniel, H. Delta-aminolevulinic acid transport by intestinal and renal peptide transporters and its physiological and clinical implications. *J. Clin. Invest.* **1998**, *101*, 2761−2767.

(33) Döring, F.; Will, J.; Amasheh, S.; Clauss, W.; Ahlbrecht, H.; Daniel, H. Minimal molecular determinants of substrates for recognition by the intestinal peptide transporter. *J. Biol. Chem.* **1998**, *273*, 23211−23218.

(34) Ganapathy, M. E.; Brandsch, M.; Prasad, P. D.; Ganapathy, V.; Leibach, F. H. Differential recognition of $\beta$-lactam antibiotics by intestinal and renal peptide transporters, PEPT 1 and PEPT 2. *J. Biol. Chem.* **1995**, *270*, 25672−25677.

(35) Ganapathy, M. E.; Prasad, P. D.; Mackenzie, B.; Ganapathy, V.; Leibach, F. H. Interaction of anionic cephalosporins with the intestinal and renal peptide transporters PEPT 1 and PEPT 2. *Biochim. Biophys. Acta* **1997**, *1324*, 296−308.

(36) Brandsch, M.; Brandsch, C.; Prasad, P. D.; Ganapathy, V.; Hopfer, U.; Leibach, F. H. Identification of a renal cell line that constitutively expresses the kidney-specific high-affinity H+/peptide cotransporter. *FASEB J.* **1995**, *9*, 1489−1496.
(37) Ganapathy, M. E.; Huang, W.; Wang, H.; Ganapathy, V.; Leibach, F. H. Valacyclovir: A substrate for the intestinal and renal peptide transporters PEPT1 and PEPT2. *Biochem. Biophys. Res. Commun.* **1998**, *246*, 470−475.
(38) Våbenø, J.; Brisander, M.; Lejon, T.; Luthman, K. Diastereoselective reduction of a chiral *N*-Boc protected *δ*-amino-α,*β*-unsaturated *γ*-keto ester Phe-Gly dipeptidomimetic. *J. Org. Chem.* **2002**, *67*, 9186−9191.
(39) Berts, W.; Luthman, K. Synthesis of a complete series of C-4 fluorinated Phe-Gly mimetics. *Tetrahedron* **1999**, *55*, 13819−13830.
(40) Deziel, R.; Plante, R.; Caron, V.; Grenier, L.; LlinasBrunet, M.; Duceppe, J. S.; Malenfant, E.; Moss, N. Practical and diastereoselective synthesis of ketomethylene dipeptide isosteres of the type AAΨ[$COCH_2$]Asp. *J. Org. Chem.* **1996**, *61*, 2901−2903.
(41) The natural dipeptides used in this study (Phe-Gly and Phe-Ala) are labile to enzymatic hydrolysis in cell culture. As there is no way to circumvent this problem, it should be kept in mind that there are potential uncertainties associated with the calculations. The possible effects on the $K_i$ values of Phe-Gly and Phe-Ala will be less pronounced in the Caco-2 assay (incubation time 5 min) than in the SKPT assay (incubation time 30 min). Regarding Gly-Pro, it has been used in several studies of PEPTX-mediated transport due to its relatively high stability (Ganapathy, V.; Mendicino, J.; Pashley, D. H.; Leibach, F. H. Carrier-mediated transport of glycyl-L-proline in renal brush border vesicles. *Biochem. Biophys. Res. Commun.* **1980**, *97*, 1133−1139).
(42) Bravo, S. A.; Nielsen, C. U.; Amstrup, J.; Frokjaer, S.; Brodin, B. Epidermal growth factor (EGF) decreases PepT2 transport capacity and expression in the rat kidney proximal tubule cell line SKPT0193 cl.2. *Am. J. Physiol. Renal Physiol.* **2003**, in press.
(43) Another explanation is that the different calculation methods used can influence the results shown in Figures 7 and 8 and hence the conclusions drawn from these results. $P_{app}$ is calculated from the linear part of the curve describing the amount of substrate transported as a function of time (eq 4) and is a steady-state value. In contrast, the apical uptake is not a steady-state value as such, since the uptake is measured under both pre-steady- and steady-state conditions (eq 3). However, the uptake experiments will still reflect the contribution from hPEPT1, and since this seems to be absent, the transepithelial transport (which suggests the contribution of hPEPT1) must be described by another mechanism.
(44) Tamura, K.; Lee, C. P.; Smith, P. L.; Borchardt, R. T. Effect of charge on oligopeptide transporter-mediated permeation of cyclic dipeptides across Caco-2 cell monolayers. *Pharm. Res.* **1996**, *13*, 1752−1754.
(45) Nielsen, C. U.; Supuran, C. T.; Scozzafava, A.; Frokjaer, S.; Steffansen, B.; Brodin, B. Transport characteristics of L-carnosine and the anticancer derivative 4-toluenesulfonylureido-carnosine in a human epithelial cell line. *Pharm. Res.* **2002**, *19*, 1337−1344.
(46) Rubio-Aliaga, I.; Daniel, H. Mammalian peptide transporters as targets for drug delivery. *Trends Pharmacol. Sci.* **2002**, *23*, 434−440.
(47) Bailey, P. D.; Boyd, C. A. R.; Bronk, J. R.; Collier, I. D.; Meredith, D.; Morgan, K. M.; Temple, C. S. How to make drugs orally active: A substrate template for peptide transporter PepT1. *Angew. Chem., Int. Ed. Engl.* **2000**, *39*, 506−508.
(48) Studies have also indicated that substrates may interact with a hydrophobic pocket in the $R_1$-position (Nielsen, C. U.; Andersen, R.; Brodin, B.; Frokjaer, S.; Taub, M. E.; Steffansen, B. Dipeptide model prodrugs for the intestinal oligopeptide transporter. Affinity for and transport via hPepT1 in the human intestinal Caco-2 cell line. *J. Controlled Release* **2001**, *76*, 129−138).
(49) It should be mentioned that there is a possibility for the involvement of the peptide transporter 1 (hPT1) in the transport of dipeptidomimetics as suggested for valaciclovir (Landowski, C. P.; Sun, D.; Foster, D. R.; Menon, S. S.; Barnett, J. L.; Welage, L. S.; Ramachandran, C.; Amidon, G. L. Gene expression in the human intestine and correlation with oral valacyclovir pharmacokinetic parameters. *J. Pharmacol. Exp. Ther.* **2003**, *306*, 778−786); however, the role of hPT1 in transport of peptides and peptidomimetics is still not well understood.
(50) Nielsen, C. U.; Amstrup, J.; Steffansen, B.; Frokjaer, S.; Brodin, B. Epidermal growth factor inhibits glycylsarcosine transport and hPepT1 expression in a human intestinal cell line. *Am. J. Physiol. Gastroint. Liver Physiol.* **2001**, *281*, G191−G199.
(51) Ouyang, H.; Tang, F.; Siahaan, T. J.; Borchardt, R. T. A modified coumarinic acid-based cyclic prodrug of an opioid peptide: Its enzymatic and chemical stability and cell permeation characteristics. *Pharm. Res.* **2002**, *19*, 794−801.
(52) Cheng, Y. C.; Prusoff, W. H. Relationship between the inhibition constant ($K_I$) and the concentration of inhibitor which causes 50% inhibition ($I_{50}$) of an enzymatic reaction. *Biochem. Pharmacol.* **1973**, *22*, 3099−3108.

JM031022+